HHS Public Access

Author manuscript

Biomaterials. Author manuscript; available in PMC 2019 May 01.

Published in final edited form as:

Biomaterials. 2018 May ; 164: 121–133. doi:10.1016/j.biomaterials.2018.02.037.

In vivo spatiotemporal dynamics of NG2 glia activity caused by neural electrode implantation

Steven M Wellman[1,2] and **Takashi DY Kozai**[1,2,3,4,5,*]

[1]Department of Bioengineering, University of Pittsburgh

[2]Center for the Basis of Neural Cognition

[3]Center for Neuroscience, University of Pittsburgh

[4]McGowan Institute of Regenerative Medicine, University of Pittsburgh

[5]NeuroTech Center, University of Pittsburgh Brain Institute

Abstract

Neural interface technology provides direct sampling and analysis of electrical and chemical events in the brain in order to better understand neuronal function and treat neurodegenerative disease. However, intracortical electrodes experience inflammatory reactions that reduce long-term stability and functionality and are understood to be facilitated by activated microglia and astrocytes. Emerging studies have identified another cell type that participates in the formation of a high-impedance glial scar following brain injury; the oligodendrocyte precursor cell (OPC). These cells maintain functional synapses with neurons and are a crucial source of neurotrophic support. Following injury, OPCs migrate toward areas of tissue injury over the course of days, similar to activated microglia. The delayed time course implicates these OPCs as key components in the formation of the outer layers of the glial scar around the implant. *In vivo* two-photon laser scanning microscopy (TPLSM) was employed to observe fluorescently-labeled OPC and microglia reactivity up to 72 hours following probe insertion. OPCs initiated extension of cellular processes (2.5 ± 0.4 μm h^{-1}) and cell body migration (1.6 ± 0.3 μm $hour^{-1}$) toward the probe beginning 12 hours after insertion. By 72 hours, OPCs became activated at a radius of about 190.3 μm away from the probe surface. This study characterized the early spatiotemporal dynamics of OPCs involved in the inflammatory response induced by microelectrode insertion. OPCs are key mediators of tissue health and are understood to have multiple fate potentials. Detailed spatiotemporal characterization of glial behavior under pathological conditions may allow identification of alternative intervention targets for mitigating the formation of a glial scar and subsequent neurodegeneration that debilitates chronic neural interfaces.

*Corresponding author: tdk18@pitt.edu.

Keywords

Glial progenitor; microelectrode array; insertion; neuroinflammation; gliosis; glial activation; ramification

1. Introduction

Communicating with the nervous system through bidirectional microelectrode arrays enhances our understanding of the brain and provides the possibility of improving the quality of life for patients who suffer from neurodegenerative disorders [1–4]. Arrays that record specific populations of neurons in the brain can provide information about neural coding that occurs during memory formation and learning in order to better understand the neural basis of cognition and physiological functions of the brain [5]. Likewise, the high spatial resolution provided by these neural interfaces has the potential to enable tetraplegic patients to control functional neuroprosthetic limbs [3, 6]. Applications involving microelectrode arrays are critically dependent on the device's ability to reliably deliver or record signals to and from electrically excitable cells over chronic periods of time. Ultimately, the goal is to develop neural technology that seamlessly integrates with biological tissue and achieves high functionality as well as long-term stability.

Implantation of a microelectrode array triggers a series of events beginning with blood-brain barrier (BBB) disruption followed by an inflammatory tissue response that has been hypothesized to impair device performance over time [7–9]. Gliosis, described as the scar formed due to the activation of microglia and astrocytes, encapsulates the microelectrode surface and creates a mechanical and chemical barrier between the device interface and neural tissue. One role of microglia is to act as resident immune cells in response to brain injury, facilitating tissue breakdown and repair through the removal of debris and secretion of inflammatory factors. Normally, microglia maintain a ramified state through the extension and retraction of processes radially around their cell body constantly surveying their surroundings for disturbances in the extracellular environment. After probe insertion, microglia in the vicinity of the insertion site preferentially extend microglial processes in the direction of the implant within the first 45 minutes and maintain relatively little cell body movement within the first 6 hours [10]. At 6 hours post-insertion, microglia appear to be activated through the observation of distinct changes in cell morphology up to a radius of about 130 μm [10]. When activated, microglia undergo an amoeboid morphology, becoming phagocytic and secreting various pro-inflammatory cytokines, chemokines, and reactive oxygen intermediates [10]. Reactive astrocytes become hypertrophic in morphology, synthesizing cytoskeletal proteins to expand their plasma membrane and form a sheath of cells around the electrode [11, 12]. The development of a glial scar progresses in the days and weeks following electrode insertion fostering a proinflammatory environment that contributes to neuronal loss, diminishing the quality of recordable activity.

NG2-expressing progenitor cells, also referred to as NG2 glia or oligodendrocyte precursor cells (OPCs), are glial cells that exist in both the developing and mature central nervous system (CNS) [13]. They represent 5-8% of all cells in the adult CNS and are distributed in a

grid-like orientation throughout gray and white matter with individual cells and processes occupying non-overlapping regions of space [14, 15]. They possess the unique glial ability to form functional synapses with neurons, allowing them to provide neurotrophic support and modulate neuronal activity [16]. These connections are bidirectional; neurons can influence NG2 glia by mediating their proliferation and differentiation via glutamatergic signaling of AMPA receptors [17]. It is hypothesized that neuronal health is dependent on the maintenance of these synaptic connections with NG2 glia. Previous studies have shown that induced ablation of NG2 glia compromises neuronal viability by inducing neuroinflammation and cell death [18, 19]. Additionally, NG2 glia are an important reservoir of oligodendrocyte progenitors for oligodendrocyte repopulation after a demyelinating injury. Oligodendrocyte cell bodies and myelin are prevalent in the cortex, albeit at lower relative densities due to the presence of neuronal cell bodies [20]. They are responsible for the mechanical and trophic support of neurons through myelin ensheathment, which is critical for the long-range propagation of action potentials [21]. For example, in the demyelinating disease multiple sclerosis, a failure of remyelination in chronic lesions is hypothesized to be attributed to the insufficiency or depletion of oligodendrocyte precursors which would precede neurodegeneration [22]. While the scale of demyelination is different, chronic implantation of intracortical microelectrodes have been shown to cause local demyelination around the implant, which could impact the local tissue microenvironment [23]. Lastly, while NG2 glia are primarily known for their role in the oligodendrocyte lineage to differentiate into mature oligodendrocytes, they are also considered polydendrocytes due to their capacity for multipotent differentiation into neurons and astrocytes [15, 24]. As a result, their mutually dependent relationship with neurons coupled with their multi-differentiating potential highlights the importance of NG2 glia behavior in both the healthy and diseased CNS.

Similar to microglia and astrocytes, NG2 glia display multi-processed, stellate-shaped morphology. They are highly proliferative cells in the brain, maintaining cell density among neighboring cells by proliferating and migrating in the event of cell loss or differentiation [14]. During embryonic development, more than 1/3 of protoplasmic astrocytes from the ventral forebrain are derived from NG2 glia [25], whereas no astrocytes are derived from NG2 glia postnatally [26]. However, differentiation of NG2 glia into astrocytes have been shown during pathological conditions such as spinal cord injury and cortical stab wound injury [27, 28], implicating their participation in the immune response to CNS injury. NG2 glia share attributes with reactive glia in the brain that suggests a complementary role in the response to tissue injury. Like microglia, NG2 glia survey their local environment through the extension of processes in response to local changes in tissue homeostasis [14, 29]. Furthermore, NG2 glia alter their morphology towards a more hypertrophied state similar to astrocytes and secrete axon-growth inhibiting factors in cases of CNS injury, such as the chondroitin sulfate proteoglycan NG2 (neural-glia antigen 2) [30]. Taken together, these recent findings have implicated NG2 glia in the formation of a glial scar and mediator of neuroinflammation following damage to the CNS. However, the dynamics of NG2 glia following intracortical microelectrode insertion has yet to be characterized.

The objective of the present study aims to uncover the spatiotemporal role of NG2 glia in the development of a barrier-forming scar, which impairs microelectrode performance by

facilitating progressive neurodegeneration. Discovering biochemical pathways that trigger the activation of glia or loss of neurons have helped improve tissue health and recording capabilities of implanted neural devices in the past [31, 32]. Traditional immunohistochemistry has been used previously to highlight patterns between different immune response biomarkers and chronically implanted electrodes. However, these methods limit the visualization of varying cellular dynamics that occur acutely during inflammation. Here, we account the use of two-photon microscopy to uncover the reactive dynamics of NG2 glia after electrode insertion *in vivo*. We observe microglia in parallel to determine temporal and spatial observations of the response between both cell types to inserted devices, possibly highlighting novel patterns in glial activity previously unknown. Identifying a temporal pattern of glial reactivity may allow targeted intervention at critical time points [31]. For example, mitigating this immune response induced by microelectrode insertion can help improve the stability and longevity of neural devices through enhanced integration with host tissue [32].

2. Methods

2.1 Surgical probe implantation

Two-photon experiments were conducted using four-shank 16-channel Michigan style silicon probes (3 mm long, 15 μm thick, 55 μm wide, 125 μm center-to-center shank spacing) mounted on non-functional tabs (NeuroNexus Technologies, Ann Arbor, MI). Electrodes were implanted into the cerebral cortex of transgenic mice (male, 22-30g, Jackson Laboratories; Bar Harbor, ME) expressing either green fluorescent protein (GFP) in NG2-glia (*Cspg4-EGFP*, n=5) or GFP in microglia cells (*CX3cr1-EGFP*, n=5). Prior to surgery animals were administered an intraperitoneal (IP) injection of 75 mg/kg ketamine and 7 mg/kg xylazine cocktail and placed in a stereotaxic frame. After removing the skin and connective tissue from the skull, a thin layer of Vetbond (3M) was applied to dry the bone and improve adhesion between the bone and headcap. Two bone screws were inserted into bone screw holes made using a high-speed dental drill over both motor cortices and secured with dental cement. A 4 mm by 6 mm craniotomy was performed over the left visual cortex centered at a point 1.5 mm rostral to lambda and 1 mm lateral from the midline. To prevent thermal damage from drilling, the skull was periodically bathed in saline. Probes were inserted through intact dura and pia in the rostral direction into the cortex at a 30° angle and parallel to the midline at 400 μm/s for a total distance of 600 μm (oil hydraulic Microdrive; MO-82, Narishige, Japan) and a final resting depth of 250-300 μm (layer II-III) beneath the surface of the brain. Effort was taken to avoid blood vessel penetration during insertion. To create a chronic imaging window, Kwik-Sil was used as a sealant inside the craniotomy before placing a glass coverslip and securing with dental cement[33]. A 2 mm tall well was formed around the imaging window to hold water for a water-immersive objective lens. Sulforhodamine 101 (SR101) was injected IP to visualize vascularization (red; 0.02-0.04 cc; 1 mg of drug per ml of sterile saline; taken from [34]). Updates of SR101 were administered approximately every hour to maintain vascular labeling. All procedures and experimental protocols were approved by the University of Pittsburgh, Division of Laboratory Animal Resources, and Institutional Animal Care and Use Committee in accordance with the standards for humane animal care as set by the

Animal Welfare Act and the National Institutes of Health Guide for the Care and Use of Laboratory Animals.

2.2 Two-Photon Imaging

In vivo imaging was performed using a two-photon laser scanning microscope as previously published [34]. The microscope consisted of a scan head (Bruker, Madison, WI), an OPO laser (Insight DS+; Spectra-Physics, Menlo Park, CA) tuned to a wavelength of 920 nm, non-descanned photomultiplier tubes (Hamamatsu Photonics KK, Hamamatsu, Shizuoka, Japan), and a 16X, 0.8 numerical aperture water immersion objective lens (Nikon Instruments, Melville, NY). During imaging, mice were anesthetized with isoflurane (1.0-1.5%, mixed with 0.9 L/min O_2) and, prior to every Z-stack, injected with Sulforhodamine 101 (SR101) for visualization of blood vessels. If an animal experienced pial surface bleeding severe enough to impact imaging quality, the animal was removed from the study. An imaging window of 407.5 × 407.5 μm (1024 × 1024 pixels) was used to visualize electrode shanks and adjacent tissue for quantification. Regions of interest were chosen by judging the two outermost shanks for the least amount of vasculature within the adjacent tissue to maximize image clarity. Z-stack images every 2 μm along the full depth of the implant were acquired at 2, 4, 6, 8, 10, 12, 24, 48 and 72 hours post-insertion with a scan rate of ~5 s/image.

2.3 Data Analysis

Image z-stacks were processed using ImageJ (National Institute of Health). In order to quantify differences in cell processes extension, soma migration, and morphology, z-stacks of consecutive time points were aligned with each other with respect to the probe. To do this, the offset position of one z-stack relative to another z-stack was determined using a “TurboReg” plugin for ImageJ. Next, the translate feature was used to align both z-stacks with each other. Cell processes and soma migration were quantified up until the point of destination at the surface of the implant. Both processes and cell body movements moving toward or away from the probe were tracked by determining XY coordinates and using the ‘Measure’ feature in ImageJ. Direction of cell processes extension and soma movement was noted by drawing a line through the center of the cell parallel to the surface of the probe. Processes extension was recorded as the distance between processes for consecutive time points while migration of cell bodies was recorded as the distance between soma for consecutive time points.

Surface coverage of NG2 glia and microglial processes along the face of the probe were measured as the percent of fluorescent signal measured over the total probe area. Each z-stack was rotated using ImageJ’s built-in plugin “Interactive Stack Rotation” to reslice the total volume of tissue normal to the probe surface. A binary mask of the sum slice projection of a small volume of tissue directly above the probe surface was created by using a built-in ImageJ thresholding method utilizing an isodata algorithm [35]. The outline of the probe was identified and the number of nonzero pixels were counted and taken as a fraction of the total area measured. The outline defined around the probe was verified to ensure correct dimensions around the probe perimeter.

Since the NG2 protein is also expressed in pericytes and macrophages as well as NG2 glia [36], examination of each tracked cell for a multi-processed morphology, a characteristic unique to NG2+ oligodendrocyte precursor cells, was confirmed before analysis. Cell morphology was characterized using morphological metrics developed previously [34]. Cells were classified as either ramified, or non-activated (1), with processes extending equally in every direction, or in a transitional (activated) stage (0), with processes orientated preferentially on one side of the soma. This morphological state was determined using the same hemispheric divide previously detailed for cell processes and soma velocity. Cells were binned based on the distance between the center of soma and the probe surface. A logistic regression was used to fit the data to show the Bernoulli Probability Distribution of cells in a ramified or transitional state (0 or 1) as a function of distance from the surface of the probe as previously published [34].

Two other metrics, the transitional index (T-index) and directionality index (D-index), were used to quantify and compare cell morphology. The T-index was calculated by measuring the length of the leading process (n), which is the longest process extending toward the probe, and the length of the longest lagging process (f), which is the process extended away from the probe at each time point. The D-index was calculated in a similar manner by counting the number of processes extending toward the probe (n) and the number of processes orientated away from the probe (f) using the hemispheric divide to distinguish between toward and away processes. The following formula was used to calculate index values for each time point:

$$\text{Index} = \frac{(f-n)}{(f+n)} + 1. \quad (1)$$

For both T-index and D-index, a measured index of 1 indicates a ramified, or non-activated, morphology while an index of 0 indicates a fully transitional, or activated, morphology with processes extending toward the surface of the probe, similar to the ramification method detailed previously [34]. After binning, cell morphology was reported as a distribution of index values as a function of distance from the probe surface. A dual sigmoidal function generated from a custom MATLAB script was used to fit this index distribution. The function required inputs of amplitude (a), shoulder location (d_1 and d_2 in μm), and shoulder width (w_1 and w_2 in μm), with the constraints maintained between 0 and 1:

$$y(d) = \frac{a}{1+e^{d-d_1/w_1}} + \frac{1-a}{1+e^{d-d_2/w_2}}. \quad (2)$$

Lastly, quantifiable changes in the vasculature over 72 hours were recorded by measuring blood vessel diameter in ImageJ. The percent change in blood vessel (b.v.) diameter was calculated as the difference between vessel diameter at the current time point and vessel diameter at 2 hours divided by the vessel diameter at 2 hours post-insertion.

2.4 Statistical Analysis

A Welch's *t*-test (unequal variance) was used to compare differences in processes extension, cell body migration, surface coverage, and morphological alterations between NG2 glia and microglia populations. To determine differences between time points within NG2 glia populations and blood vessel z-stacks, a repeated measures analysis of variance (ANOVA) was used. A $p < 0.05$ was chosen to demonstrate significant differences.

3. Results

Prior to insertion, the distribution of NG2 glia and microglia was uniform and no morphological changes were observed across the cortex due to the craniotomy. A probe was inserted at an angle into the cortex and sealed by a chronic imaging window that allows for two-photon visualization of fluorescently labeled glial cells (Figure 1a). Due to the physical constraints of two-photon microscopy, observations of the tissue response around electrodes traditionally inserted perpendicularly to the brain are difficult and the extent of these limitations have been addressed in a previous publication [10]. Large surface vasculature was avoided during insertion to minimize bleeding and proper sealing methods were used to preserve the region of interest in the tissue during chronic imaging [7, 31, 33]. Laser and PMT settings were set to the lowest settings necessary to prevent thermal damage while imaging. A region of interest 300 μm adjacent to the probe shank was chosen for quantification (Figure 1b-c). Vascular bound pericytes also express the NG2 antigen and therefore were fluorescently labeled by the transgenic model. These pericytes maintain distinct morphological characteristics that are distinguishable from NG2+ oligodendrocyte progenitors and were not included in the analysis (Figure 1d). Additionally, the literature indicates that pericytes experience a rapid decrease in number following trauma to the brain, while pericyte migration or pericytosis around the lesion does not occur until 3-5 days post-injury [37, 38]. Therefore, it is not expected to observe any migrating GFP-labeled pericytes given the timeframe of analysis. Furthermore, proliferating NG2 glia can be mistaken as activated cells that are morphologically distinct from the ramified state; however, they can be easily identified as a pair of two NG2 glia cells migrating in opposite directions and thus were also excluded from quantification (Figure 1e). Fluorescently-labeled NG2 glia and microglia were observed every 2 hours for the first 12 hours and 24, 48, and 72 hours following electrode insertion. Sulforhodamine 101 was administered intraperitoneally to observe changes in the vasculature.

3.1 NG2 glia begin cellular processes extension between 12 to 24 hours following electrode insertion

NG2 glia react first through the extension of processes toward the surface of the probe (Figure 2a). Processes on the soma opposite to the probe surface are retracted and processes facing the implantation site are extended. As a result, the soma of NG2 glia appear elongated along this direction. There was no observable movement in NG2 glia cell processes for the first 12 hours following insertion (Figure 2b). After 12 hours, NG2 glia processes moved at a rate of about 2.5 ± 0.4 μm h^{-1} toward the direction of the electrode before decreasing over the next 48 hours (Figure 2c). Velocities were no longer quantified once cell processes reached their destination (probe surface). In comparison, microglia extend cellular processes

immediately following electrode insertion, with most extensions occurring within the first hour following injury. NG2 glia process velocities were significantly different than microglia processes at 12 hours post-insertion when NG2 glia begin to initiate changes in cell polarity (Welch's T-test; $p < 0.05$; Supplementary Table 1). Interestingly, while microglia processes move at the rate of microns per minute, NG2 glia processes move at rate of microns per hour, considerably slower than microglia.

3.2 NG2 glia migrate toward the probe surface shortly after extension of processes

Cell body migration of NG2 glia toward the surface of the device begins 12 to 24 hours following insertion (Figure 3a). Likewise, microglia did not show any discernable locomotion in the first 10 hours once their processes contacted the probe surface within the first hour of insertion (Figure 3b). NG2 glia cell bodies migrate at a rate of 1.6 ± 0.3 μm $hour^{-1}$ while microglia migrate at a rate of 2.1 ± 0.3 μm $hour^{-1}$. No significant differences were found for cell body migration velocities between NG2 glia and microglia (Welch's T-test; $p > 0.05$; Supplementary Table 2) (Figure 3c). Similarly, when observed as a function of distance from the probe surface, there were no significant differences ($p > 0.05$; Supplementary Table 3) in cell migration velocities between different distances of the cell relative to the probe as well as between NG2 glia and microglia (Figure 3d). Since no NG2 glia were seen activated near 300 μm from the probe surface, quantification of cell body velocity of NG2 glia was not permitted within this region. Additionally, both NG2 glia and microglia increase in coverage over the surface of the probe from 2 to 72 hours post-insertion (Figure 4a) using previously published methods [34]. The percent of tissue labeled with GFP-fluorescence increased significantly for each cell type over time from 36.3 ± 4.2% to 72.6 ± 8.9% for NG2 glia (Welch's T-test; $p < 0.05$; Supplementary Table 4) and from 52.8 ± 4.5% to 91.4 ± 3.3% for microglia ($p < 0.05$) (Figure 4b). At 2 hours, microglia coverage was significantly increased compared to NG2 glia ($p < 0.05$). However, NG2 glial coverage did not differ significantly from microglia at 72 hours post-insertion ($p > 0.05$).

3.3 Ramified NG2 glia become activated over time with distance from the electrode

NG2 glia were classified as either ramified (R) or transitional (T) through visual observation of the orientation of their processes on either side of an imaginary line drawn through their cell soma parallel to the surface of the implant (Figure 5a). NG2 glia transform from a ramified to activated morphology beginning 12 hours after insertion. At 72 hours, NG2 glia were activated at a radius of about 190.3 μm away from the probe surface (Figure 5b). Characterization of their leading and lagging processes relative to the injury showed that NG2 glia begin extending processes toward the probe surface while retracting processes which are orientated away from the opposite direction (Figure 5c). Gradually, the number of processes facing away from the probe begin to reduce as NG2 glia begin to alter cell polarity and extend processes toward the direction of the implant (Figure 5d). In comparison, microglia are activated up to a distance of 105.6 μm beginning 2 hours after insertion and by 72 hours they are activated at least 300 μm away from the probe surface, spanning the fully imaged region of interest (Figure 6a). Over time, lagging microglia processes begin to shorten and reduce as more leading processes lengthen in the direction of the probe which were quantified as T-index and D-index (Figure 6b-c).

3.4 Activation radius of NG2 glia 72 hours following probe insertion

NG2 glia and microglia share a number of morphological similarities and differences in ramified and activated states. Both glia processes extend radially about their somas while ramified; however, NG2 glia processes appear long and thin while microglia processes are short, more highly branched, and bulbous at the tips (Figure 7a). When activated, each glia orientates processes in a preferred direction relative to their cell bodies. However, large temporal differences were observed between NG2 and microglia activation. Two hours post-insertion, all nearby NG2 glia remain ramified while microglia become activated up to a distance of 105.6 μm (Figure 7b). Within this radius, microglia were significantly more activated than NG2 glia (Welch's T-test; $p < 0.05$; Supplementary Table 7). No significant differences ($p > 0.05$) were noted in the activation patterns of NG2 glia and microglia 12 hours following insertion (Figure 7c). At 72 hours post-insertion, ramified NG2 glia can still be observed greater than 200 μm from the electrode while nearly all microglia within a 300 μm radius were observed to be in an activated state (Figure 7d). Microglia beyond 200 μm were significantly more activated than NG2 glia at 72 hours post-insertion ($p < 0.05$).

3.5 Dynamic vasculature changes after insertion injury

Venuoles within the vicinity of the probe experienced increases in vessel diameter over the course of 72 hours following insertion (Figure 8a). Venuoles can be easily identified from arterioles and capillaries due to the distinct lack of NG2+ smooth muscle cells and pericytes, respectively [39, 40]. Quantifying the change in blood vessel diameter over time (taken as the percentage of the change in vessel diameter from 2 hours post-insertion) showed a significant difference in vessel size between 12 and 24 hours post-insertion (repeated ANOVA; $p < 0.01$; Supplementary Table 8) and 24 and 48 hours post-insertion ($p < 0.001$). On average, venuoles increased by 50% of their original size around the probe (Figure 8b). Figure 8a shows an extreme scenario where one venuole nearly tripled in vessel diameter. Interestingly, arterioles did not show any noticeable differences in diameter over the 72 hour period. Furthermore, NG2 glia were observed to respond to vasculature events (Figure 8c).

4. Discussion

Under normal physiological conditions, NG2 glia exist as a distinct glial population in the brain, with numerous roles including acting as precursors to myelinating oligodendrocytes and providing neurotrophic support to neurons through synaptic connections. They extend and retract processes radially around their cell bodies constantly surveying their extracellular environment [14]. However, unlike microglia who display a few short processes with bulbous endings, NG2 glia maintain numerous long, thin processes around their cell soma. During injury, NG2 glia are highly proliferative and widely distributed across the brain, hold astrogliogenic potential, and can secrete axon-growth inhibitory factors [41]. Electrode insertion into the brain induces a graded inflammatory response beginning with blood-brain barrier disruption, which leads to infiltration of blood-borne leukocytes/macrophages, complement system activation, edema, and plasma protein exposure to neuronal and glial cells [42]. Activation of microglia (within minutes) and astrocytes (within days) elicits a change in their behavior and morphology as they initiate glial scar formation around the device and secrete cytokines and chemokines which affect other glial cells, neurons, and

BBB permeability. NG2 glia have reportedly been implicated in glial scar formation following brain injury [14, 43]. Here we demonstrate a temporal and spatial sequence of NG2 glia activation around inserted probes using two-photon microscopy to track processes extension, cell body migration, and quantifiable changes in cell morphology. NG2 glia responses to the presence of the probe are characteristically similar to the behavior previously reported for microglia cells. However, the reaction observed from NG2 glia occurs hours following injury as opposed to microglia which react within minutes.

4.1 NG2 glia do not respond to insertion injury within the first 12 hours

NG2 glia have been shown previously to react to brain injury, both in response to the death of individual NG2 glia [14] and large-scale lesions such as spinal cord injury and stroke [44, 45]. Along with microglia, they are the first cells to proliferate within 24 hours following injury, whereas astrocytes proliferate days later [46]. Previously, it has been shown that microglia activate immediately upon insertion via the extension of cellular processes toward the probe surface [10]. Here we observe that NG2 glia do not undergo changes in cell morphology within the first 12 hours following probe insertion. This is confirmed by the observation of equal length processes in all radial directions around their cell bodies as well as the lack of a hypertrophic cell shape that is a characteristic of activated glia. Following 12 hours after insertion, NG2 glia begin to preferentially extend their processes in the direction of the probe at a rate of 2.5 ± 0.4 μm h^{-1}, similar to what has been reported previously (2.7 ± 0.4 μm h^{-1}) [14]. In contrast, microglia processes extend at a rate of 1.6 ± 1.3 μm min^{-1} and terminate on the probe surface within the first hour following insertion [47]. This results in spatially distinct layers of microglia processes surrounded by NG2 glia processes within the glia scar [14].

4.2 NG2 glia migrate cell bodies toward the surface of the device shortly after activation

Within 24 hours after CNS injury, a rapid increase in NG2+ expression is observed around the implant site [48, 49]. Here we show that NG2 glia migrate toward the surface of the probe shortly following processes extension at 12 hours post-insertion. NG2 glia migrate toward the probe at a rate of 1.6 ± 0.3 μm $hour^{-1}$, which did not differ significantly ($p = 0.3219$) from the rate of microglia migration (2.1 ± 0.3 μm $hour^{-1}$) indicating the velocity of cell body movement is not intrinsic to either individual glial cell. Currently, the circumstances surrounding NG2 activation, and thus migration and proliferation, during glial scar formation is relatively unknown. It is known that microglia become activated when exposed to inflammatory plasma proteins that are released following blood-brain barrier permeability, explaining their immediate reaction to the disruption of vasculature from inserted microelectrodes [50, 51]. Cytokine gradients that are produced following injury may explain the graded increase in cell activation over time as a function of distance from the implant [52]. NG2 produced in NG2 glia is known to direct migration and orientation by regulating cell polarity via fibroblast growth factor (FGF)-dependent activation of the RhoA/ROCK pathway [53]. FGF production is observed in CNS injuries such as multiple sclerosis (MS) and cortical stab wounds [54–56] and it is important for wound healing and angiogenesis after blood vessel injury [57]. Thus, severity of blood-brain barrier disruption could lead to the upregulation of chemotactic FGF, recruiting NG2 glia and other immune cells to the implant injury site. Other factors which influence NG2 glia migration as well as

proliferation are platelet-derived growth factor (PDGF) and chemokines CXCL1, CXCR4, CXCL12, and CCL11 [58–60].

After NG2 glia and microglia cells extended processes and migrated cell bodies towards the probe, the glial cells began encapsulating the probe indicating interaction between the glial cells and the implant (a foreign body). At 2 hours post-insertion, microglia covered 52.8 ± 4.5% of the probe surface, similar to what was reported previously (47.7% ± 3.4%) [34]. NG2 glia coverage differed significantly from microglia coverage at 2 hours following implantation, which is expected given that microglia extension of processes begins within the first hour following insertion while NG2 glia do not respond until after 12 hours post-insertion. Over the course of 72 hours, both microglia and NG2 glia significantly increased in coverage over the probe surface reflecting their parallel migration toward the device over this time period. However, it is not clear to what extent is this surface coverage the result of glial cell migration to the probe or proliferation at the lesion site, given that both NG2 glia and microglia significantly proliferate within the following days after acute injury to the brain [61]. At 72 hours post-insertion, NG2 glia doubled the amount of surface coverage within this period resulting in no significant difference from microglial coverage. Additional longitudinal studies are needed to determine if NG2 glia coverage would continue to increase in surface coverage beyond 72 hours of implantation.

4.3 Activated NG2 glia undergo morphological changes following insertion injury

After injury, NG2 glia cell bodies begin to hypertrophy as their cytoskeletal structure rearranges and prepares for movement, similar to microglia and astrocytes during the formation of a glial scar [62]. NG2 glia activated from a normal ramified morphology 12 hours after probe insertion. A distribution of NG2 glia ramification as a function of distance from the surface of the probe was generated by assigning an index value of either 0 for transitional, or activated, morphology or 1 for a ramified morphology. NG2 glia became activated up to a distance of 190.3 μm from the probe surface after 72 hours. In other words, at 72 hours, the probability that 50% or more of NG2 glia will be polarized will occur within a radius of 190.3 μm from the surface of the probe. At this time, all microglia observed within a 300 μm radius of the probe were activated. While the ramification index provided an indication of the extent of activation of NG2 glia or microglia, it lacked information about the specific orientation of the cell. This information was given by the T-index (transitional state) and D-index (directionality). Over time, both NG2 glia and microglia began to extend leading processes further toward the implant while retracting lagging processes that were orientated away from the implant (T-index = 0). Likewise, NG2 glia and microglia began preferentially orientating most of their processes in the direction of the implant (D-index = 0). These metrics allowed characterization of the preference for glia to respond to the presence of the device as opposed to responding to other insults in the brain, such as neuronal or glial cell death or disruptions of distant vasculature, reflected by a T-index or D-index greater than 1.

4.4 Changes in the vasculature around implanted probes in the brain

Electrode insertion inevitably impacts the integrity of the blood-brain barrier, either through direct disruption of vasculature or through the inflammation-induced upregulation of cellular

pathways that influence its permeability [42, 63]. Dynamic changes to the vasculature occurred 24-48 hours following injury, where venuoles increased in diameter around the probe site. The change in blood vessel diameter differed significantly with a 12.5 ± 3.1% increase in diameter at 24 hours and 45.3 ± 6.9% increase at 48 hours following insertion. It remains to be investigated if venuoles dilate in order to redirect blood flow from damaged capillary networks, accommodate additional traffic from glial cells clearing debris and waste products, or alleviate increases in drainage pressure. Interestingly, no appreciable differences were observed in arteriole size over 72 h in the animals in this study. NG2 glia were observed proximal to these vascular events near the inserted probe. However, it is unclear whether they were responding to the changes to the blood vessel or were merely being pushed away by the rapidly expanding vascular membrane. Regardless, functional analysis showed that NG2 glia play a role in maintaining BBB integrity through the release of TGF-β1, a factor that induces extracellular matrix production in pericytes [64]. Pericytes express platelet-derived growth factor beta (PDGFR-β) as well as the NG2 antigen and therefore can be observed using the *Cspg4-EGFP* transgenic mouse model. However, they were excluded since this study focused on NG2+ oligodendrocyte precursor cells. These pericytes are visually distinct from NG2 glia in morphology and position in the cortex, normally residing along capillary walls as opposed to freely roaming within the parenchyma [65]. Besides regulation of blood flow, pericytes are also responsible for clearance of metabolic waste products from the parenchyma and mediating angiogenesis [66], and therefore are of great interest for future studies.

4.5 Future directions

One of the roles of NG2 glia in the central nervous system is to act as a reservoir of precursor cells that differentiate into myelinating oligodendrocytes after a demyelinating insult [67]. Although the extent of oligodendrocyte cell death has not been investigated in the context of microelectrode implantation, demyelinated axons have been anecdotally observed around the insertion site [68]. It is possible that NG2 glia who migrate toward the surface of the probe are responding to damaged myelin and oligodendrocytes within the area and compensate for the loss of myelinating cells by differentiating into mature oligodendrocytes. Likewise, NG2 glia are also known to have astrogliogenic potential. Similar to astrocytes, they are derived from radial glia during development, display stellate morphology, and express ion channels and receptors for neurotransmitters secreted by neurons [69, 70]. Differentiation of NG2 glia into astrocytes has been shown under *in vitro* conditions; and have been implicated as differentiating into astrocytes at the lesion sites to form part of the glial scar [27, 71, 72]. While NG2 glia differentiation into astrocytes has been observed during specific injury to the cerebral cortex such as during cryoinjury as well as focal cerebral ischemia, the extent of NG2 glia contribution to the increase in expression of glial fibrillary acidic protein (GFAP) observed around chronically implanted microelectrodes remains to be elucidated [73]. A longer timescale study is necessary to identify the spatiotemporal dynamics between astroglial scar formation and differentiation of NG2 glia into astrocytes or myelinating oligodendrocytes (oligodendrogenesis). However, detailed studies tracking oligodendrocyte progenitor differentiation into astrocytes or oligodendrocytes *in vivo* have been difficult due to the fact that differentiating NG2 glia lose antigenic markers that are targeted using immunohistochemistry techniques, such as NG2+

and PDGFRα+, as well as during *in vivo* imaging. For example, Hughes et al. observed a decrease in GFP fluorescence when oligodendrocyte precursor cells began to differentiate into oligodendrocytes as the *Cspg4* promoter was down regulated [74]. Tracking the differentiation of NG2 glia using fate-independent markers could help determine contribution of NG2 glia during injury. Ultimately, understanding the purpose for NG2 migration and proliferation around the inserted probe will provide insight as to whether the cell is participating in tissue degeneration or repair.

A unique characteristic that is not observed in other glial cells such as microglia and astrocytes is the ability for NG2 glia to provide metabolic support and neuronal modulation by establishing synaptic contacts with neurons [16]. However, additional studies are necessary to characterize the impact of NG2 glia on neuronal viability. Furthermore, it has been shown that oligodendrogenesis is regulated through neuronal signaling in which electrical depolarizations via AMPA receptors on NG2 glia induce oligodendrocyte differentiation [75]. In addition, chemical ablation of NG2 glia has been shown to lead to increased neuronal loss [19]. It is possible these connections could be compromised during injury in which NG2 glia are preferentially activating and migrating in response to the presence of an implanted microelectrode. This activation may require NG2+ cells to abandon their supportive roles under their ramified state. As a result, an increase in NG2 glial cell activation around microelectrodes could impair neuronal health and ultimately the recording and stimulating performance of neural devices. However, it has been shown that NG2 glia can be manipulated to produce new neurons following traumatic injury due to their inherent neurogenic potential [76]. In fact, previous studies have demonstrated that it is possible to observe neural progenitor cells near chronically implanted microelectrodes [11]. Guiding differentiation of these progenitors cells or chemically reprogramming glial cells into neurons may be one approach to repair brain injuries [77]. Utilizing the cell's natural machinery to convert reactive glia into functionally integrated neurons could attenuate and potentially reverse the pro-inflammatory, tissue degrading microenvironment surrounding inserted devices leading to improved chronically implantable neural interfaces.

5. Conclusion

The current study is novel in that, for the first time, it characterized the spatiotemporal activity of NG2 OPC glia participation during the inflammatory response caused by implantation of microelectrode arrays in the cortex. Two-photon microscopy techniques allow for the observation and enhanced characterization of acute NG2 glia activation 72 hours after insertion. Beginning 12 hours following insertion, NG2 glia become activated by extending cellular processes and migrating toward the surface of the device. Using previously characterized microglia cells as comparison, NG2 glia activate in a similar, yet delayed, fashion. This work enhances our understanding of the cellular and subcelluar changes that occur following injury and provides a time course of dynamic behavior that can be targeted in future interventions seeking to attenuate the activation of glial cells around implanted devices. Understanding the impact NG2 glia have on the functional performance of inserted microelectrodes could shift the focus of current efforts to improve the stability and functionality of chronically implanted neural interfaces.

Supplementary Material

Refer to Web version on PubMed Central for supplementary material.

Acknowledgments

This work was supported by NIH NINDS R01NS094396.

References

1. Cogan SF, et al. Tissue damage thresholds during therapeutic electrical stimulation. Journal of neural engineering. 2016; 13(2):021001. [PubMed: 26792176]
2. Kipke DR, et al. Advanced neurotechnologies for chronic neural interfaces: new horizons and clinical opportunities. The Journal of neuroscience : the official journal of the Society for Neuroscience. 2008; 28(46):11830–8. [PubMed: 19005048]
3. Schwartz AB, et al. Brain-controlled interfaces: movement restoration with neural prosthetics. Neuron. 2006; 52(1):205–20. [PubMed: 17015237]
4. Salatino JW, et al. Glial responses to implanted electrodes in the brain. Nature BME. 2017
5. Huber D, et al. Multiple dynamic representations in the motor cortex during sensorimotor learning. Nature. 2012; 484(7395):473–8. [PubMed: 22538608]
6. Collinger JL, et al. High-performance neuroprosthetic control by an individual with tetraplegia. Lancet. 2013; 381(9866):557–64. [PubMed: 23253623]
7. Kozai TDY, et al. Reduction of neurovascular damage resulting from microelectrode insertion into the cerebral cortex using in vivo two-photon mapping. J Neural Eng. 2010; 7(4):046011. [PubMed: 20644246]
8. Saxena T, et al. The impact of chronic blood-brain barrier breach on intracortical electrode function. Biomaterials. 2013; 34(20):4703–13. [PubMed: 23562053]
9. Goss-Varley M, et al. Microelectrode implantation in motor cortex causes fine motor deficit: Implications on potential considerations to Brain Computer Interfacing and Human Augmentation. Sci Rep. 2017; 7(1):15254. [PubMed: 29127346]
10. Kozai TD, et al. In vivo two-photon microscopy reveals immediate microglial reaction to implantation of microelectrode through extension of processes. J Neural Eng. 2012; 9(6):066001. [PubMed: 23075490]
11. Kozai TD, et al. Chronic tissue response to carboxymethyl cellulose based dissolvable insertion needle for ultra-small neural probes. Biomaterials. 2014; 35(34):9255–68. [PubMed: 25128375]
12. Szarowski DH, et al. Brain responses to micro-machined silicon devices. Brain Res. 2003; 983(1-2):23–35. [PubMed: 12914963]
13. Dawson MRL, et al. NG2-expressing glial progenitor cells: an abundant and widespread population of cycling cells in the adult rat CNS. Molecular and cellular neurosciences. 2003; 24(2):476–88. [PubMed: 14572468]
14. Hughes EG, et al. Oligodendrocyte progenitors balance growth with self-repulsion to achieve homeostasis in the adult brain. Nat Neurosci. 2013; 16(6):668–76. [PubMed: 23624515]
15. Nishiyama A, et al. Polydendrocytes (NG2 cells): multifunctional cells with lineage plasticity. Nature reviews Neuroscience. 2009; 10(1):9–22. [PubMed: 19096367]
16. Sakry D, et al. Oligodendrocyte precursor cells modulate the neuronal network by activity-dependent ectodomain cleavage of glial NG2. PLoS biology. 2014; 12(11):e1001993. [PubMed: 25387269]
17. Gautier HO, et al. Neuronal activity regulates remyelination via glutamate signalling to oligodendrocyte progenitors. Nat Commun. 2015; 6:8518. [PubMed: 26439639]
18. Nakano M, et al. NG2 glial cells regulate neuroimmunological responses to maintain neuronal function and survival. Sci Rep. 2017; 7:42041. [PubMed: 28195192]

19. Birey F, et al. Genetic and Stress-Induced Loss of NG2 Glia Triggers Emergence of Depressive-like Behaviors through Reduced Secretion of FGF2. Neuron. 2015; 88(5):941–956. [PubMed: 26606998]
20. Tomassy GS, et al. Distinct profiles of myelin distribution along single axons of pyramidal neurons in the neocortex. Science. 2014; 344(6181):319–24. [PubMed: 24744380]
21. Fields RD. Oligodendrocytes Changing the Rules: Action Potentials in Glia and Oligodendrocytes Controlling Action Potentials. The Neuroscientist: a review journal bringing neurobiology, neurology and psychiatry. 2008; 14(6):540–543.
22. Xu JP, Zhao J, Li S. Roles of NG2 glial cells in diseases of the central nervous system. Neuroscience bulletin. 2011; 27(6):413–21. [PubMed: 22108818]
23. Winslow BD, et al. A comparison of the tissue response to chronically implanted Parylene-C-coated and uncoated planar silicon microelectrode arrays in rat cortex. Biomaterials. 2010
24. Kondo T, Raff M. Oligodendrocyte precursor cells reprogrammed to become multipotential CNS stem cells. Science (New York, N Y). 2000; 289(5485):1754–7.
25. Zhu X, Hill RA, Nishiyama A. NG2 cells generate oligodendrocytes and gray matter astrocytes in the spinal cord. Neuron glia biology. 2008; 4(1):19–26. [PubMed: 19006598]
26. Rivers LE, et al. PDGFRA/NG2 glia generate myelinating oligodendrocytes and piriform projection neurons in adult mice. Nature neuroscience. 2008; 11(12):1392–401. [PubMed: 18849983]
27. Komitova M, et al. NG2 cells are not a major source of reactive astrocytes after neocortical stab wound injury. Glia. 2011; 59(5):800–9. [PubMed: 21351161]
28. Hackett AR, et al. STAT3 and SOCS3 regulate NG2 cell proliferation and differentiation after contusive spinal cord injury. Neurobiology of disease. 2016; 89:10–22. [PubMed: 26804026]
29. Hill RA, et al. Modulation of oligodendrocyte generation during a critical temporal window after NG2 cell division. Nature neuroscience. 2014; 17(11):1518–27. [PubMed: 25262495]
30. Levine JM. Increased expression of the NG2 chondroitin-sulfate proteoglycan after brain injury. The Journal of neuroscience: the official journal of the Society for Neuroscience. 1994; 14(8): 4716–30. [PubMed: 8046446]
31. Kozai TDY, et al. Dexamethasone retrodialysis attenuates microglial response to implanted probes in vivo. Biomaterials. 2016; 87:157–169. [PubMed: 26923363]
32. Kozai TD, et al. Effects of caspase-1 knockout on chronic neural recording quality and longevity: insight into cellular and molecular mechanisms of the reactive tissue response. Biomaterials. 2014; 35(36):9620–34. [PubMed: 25176060]
33. Kozai TDY, et al. Two-photon imaging of chronically implanted neural electrodes: Sealing methods and new insights. Journal of Neuroscience Methods. 2016; 256:46–55.
34. Eles JR, et al. Neuroadhesive L1 coating attenuates acute microglial attachment to neural electrodes as revealed by live two-photon microscopy. Biomaterials. 2017; 113:279–292. [PubMed: 27837661]
35. Picture Thresholding Using an Iterative Selection Method. IEEE Transactions on Systems, Man, and Cybernetics. 1978; 8(8):630–632.
36. Jones LL, et al. NG2 Is a Major Chondroitin Sulfate Proteoglycan Produced after Spinal Cord Injury and Is Expressed by Macrophages and Oligodendrocyte Progenitors. The Journal of Neuroscience. 2002; 22(7):2792. [PubMed: 11923444]
37. Zehendner CM, et al. Traumatic brain injury results in rapid pericyte loss followed by reactive pericytosis in the cerebral cortex. Scientific Reports. 2015; 5:13497. [PubMed: 26333872]
38. Fernández-Klett F, et al. Early loss of pericytes and perivascular stromal cell-induced scar formation after stroke. Journal of Cerebral Blood Flow & Metabolism. 2013; 33(3):428–439. [PubMed: 23250106]
39. Ampofo E, et al. The regulatory mechanisms of NG2/CSPG4 expression. Cellular & molecular biology letters. 2017; 22:4. [PubMed: 28536635]
40. Chan-Ling T, Hughes S. NG2 can be used to identify arteries versus veins enabling the characterization of the different functional roles of arterioles and venules during microvascular network growth and remodeling. Microcirculation (New York, N Y: 1994). 2005; 12(7):539–40. author reply 540-1.

41. Dimou L, Gallo V. NG2-glia and their functions in the central nervous system. Glia. 2015; 63(8): 1429–51. [PubMed: 26010717]
42. Kozai TD, et al. Brain tissue responses to neural implants impact signal sensitivity and intervention strategies. ACS Chem Neurosci. 2015; 6(1):48–67. [PubMed: 25546652]
43. Hackett AR, Lee JK. Understanding the NG2 Glial Scar after Spinal Cord Injury. Front Neurol. 2016; 7:199. [PubMed: 27895617]
44. Buss A, et al. NG2 and phosphacan are present in the astroglial scar after human traumatic spinal cord injury. BMC Neurol. 2009; 9:32. [PubMed: 19604403]
45. Song FE, et al. Roles of NG2-glia in ischemic stroke. CNS Neurosci Ther. 2017; 23(7):547–553. [PubMed: 28317272]
46. Simon C, Gotz M, Dimou L. Progenitors in the adult cerebral cortex: cell cycle properties and regulation by physiological stimuli and injury. Glia. 2011; 59(6):869–81. [PubMed: 21446038]
47. Kozai TDY, et al. In vivo two photon microscopy reveals immediate microglial reaction to implantation of microelectrode through extension of processes. J Neural Eng. 2012; 9
48. Fitch MT, Silver J. Glial cell extracellular matrix: boundaries for axon growth in development and regeneration. Cell Tissue Res. 1997; 290(2):379–84. [PubMed: 9321701]
49. Lemons ML, Howland DR, Anderson DK. Chondroitin sulfate proteoglycan immunoreactivity increases following spinal cord injury and transplantation. Exp Neurol. 1999; 160(1):51–65. [PubMed: 10630190]
50. Ralay Ranaivo H, Wainwright MS. Albumin activates astrocytes and microglia through mitogen-activated protein kinase pathways. Brain research. 2010; 1313:222–31. [PubMed: 19961838]
51. Adams RA, et al. The fibrin-derived gamma377-395 peptide inhibits microglia activation and suppresses relapsing paralysis in central nervous system autoimmune disease. J Exp Med. 2007; 204(3):571–82. [PubMed: 17339406]
52. Fan Y, Xie L, Chung CY. Signaling Pathways Controlling Microglia Chemotaxis. Mol Cells. 2017; 40(3):163–168. [PubMed: 28301917]
53. Biname F, et al. NG2 regulates directional migration of oligodendrocyte precursor cells via Rho GTPases and polarity complex proteins. J Neurosci. 2013; 33(26):10858–74. [PubMed: 23804106]
54. Clemente D, et al. FGF-2 and Anosmin-1 are selectively expressed in different types of multiple sclerosis lesions. The Journal of neuroscience: the official journal of the Society for Neuroscience. 2011; 31(42):14899–909. [PubMed: 22016523]
55. do Carmo Cunha J, et al. Responses of reactive astrocytes containing S100beta protein and fibroblast growth factor-2 in the border and in the adjacent preserved tissue after a contusion injury of the spinal cord in rats: implications for wound repair and neuroregeneration. Wound repair and regeneration: official publication of the Wound Healing Society [and] the European Tissue Repair Society. 2007; 15(1):134–46.
56. Robel S, Berninger B, Gotz M. The stem cell potential of glia: lessons from reactive gliosis. Nature reviews Neuroscience. 2011; 12(2):88–104. [PubMed: 21248788]
57. Lin TN, et al. Induction of basic fibroblast growth factor (bFGF) expression following focal cerebral ischemia. Brain research Molecular brain research. 1997; 49(1-2):255–65. [PubMed: 9387885]
58. Dziembowska M, et al. A role for CXCR4 signaling in survival and migration of neural and oligodendrocyte precursors. Glia. 2005; 50(3):258–69. [PubMed: 15756692]
59. Maysami S, et al. Oligodendrocyte precursor cells express a functional chemokine receptor CCR3: implications for myelination. Journal of neuroimmunology. 2006; 178(1-2):17–23. [PubMed: 16828880]
60. Tsai HH, et al. The chemokine receptor CXCR2 controls positioning of oligodendrocyte precursors in developing spinal cord by arresting their migration. Cell. 2002; 110(3):373–83. [PubMed: 12176324]
61. Susarla, Bala T., et al. Temporal patterns of cortical proliferation of glial cell populations after traumatic brain injury in mice. ASN NEURO. 2014; 6(3):e00143. [PubMed: 24670035]
62. Hansson E. Actin filament reorganization in astrocyte networks is a key functional step in neuroinflammation resulting in persistent pain: novel findings on network restoration. Neurochemical research. 2015; 40(2):372–9. [PubMed: 24952067]

63. Kozai TDY, et al. Reduction of neurovascular damage resulting from microelectrode insertion into the cerebral cortex using in vivo two-photon mapping. Journal of neural engineering. 2010; 7(4): 046011. [PubMed: 20644246]

64. Seo JH, et al. Oligodendrocyte precursor cells support blood-brain barrier integrity via TGF-beta signaling. PloS one. 2014; 9(7):e103174. [PubMed: 25078775]

65. Attwell D, et al. What is a pericyte? Journal of cerebral blood flow and metabolism: official journal of the International Society of Cerebral Blood Flow and Metabolism. 2016; 36(2):451–5.

66. Winkler EA, Bell RD, Zlokovic BV. Central nervous system pericytes in health and disease. Nat Neurosci. 2011; 14(11):1398–1405. [PubMed: 22030551]

67. Tripathi RB, et al. NG2 glia generate new oligodendrocytes but few astrocytes in a murine experimental autoimmune encephalomyelitis model of demyelinating disease. The Journal of neuroscience: the official journal of the Society for Neuroscience. 2010; 30(48):16383–90. [PubMed: 21123584]

68. Winslow BD, et al. A comparison of the tissue response to chronically implanted Parylene-C-coated and uncoated planar silicon microelectrode arrays in rat cortex. Biomaterials. 2010; 31(35): 9163–72. [PubMed: 20561678]

69. Nishiyama A, Yang Z, Butt A. Astrocytes and NG2-glia: what's in a name? Journal of anatomy. 2005; 207(6):687–93. [PubMed: 16367796]

70. Bergles DE, Richardson WD. Oligodendrocyte Development and Plasticity. Cold Spring Harbor perspectives in biology. 2015; 8(2):a020453. [PubMed: 26492571]

71. Tatsumi K, et al. Genetic fate mapping of Olig2 progenitors in the injured adult cerebral cortex reveals preferential differentiation into astrocytes. Journal of neuroscience research. 2008; 86(16): 3494–3502. [PubMed: 18816798]

72. Tatsumi K, et al. Characterization of cells with proliferative activity after a brain injury. Neurochem Int. 2005; 46(5):381–9. [PubMed: 15737436]

73. Martin V, et al. A single-cell analysis reveals multiple roles of oligodendroglial lineage cells during post-ischemic regeneration. Glia. n/a-n/a.

74. Hughes EG, et al. Oligodendrocyte progenitors balance growth with self-repulsion to achieve homeostasis in the adult brain. Nat Neurosci. 2013; 16(6):668–676. [PubMed: 23624515]

75. Gibson EM, et al. Neuronal activity promotes oligodendrogenesis and adaptive myelination in the mammalian brain. Science (New York, N Y). 2014; 344(6183):1252304.

76. Heinrich C, et al. Sox2-mediated conversion of NG2 glia into induced neurons in the injured adult cerebral cortex. Stem cell reports. 2014; 3(6):1000–14. [PubMed: 25458895]

77. Wang LL, Zhang CL. Engineering new neurons: in vivo reprogramming in mammalian brain and spinal cord. Cell and tissue research. 2018; 371(1):201–212. [PubMed: 29170823]

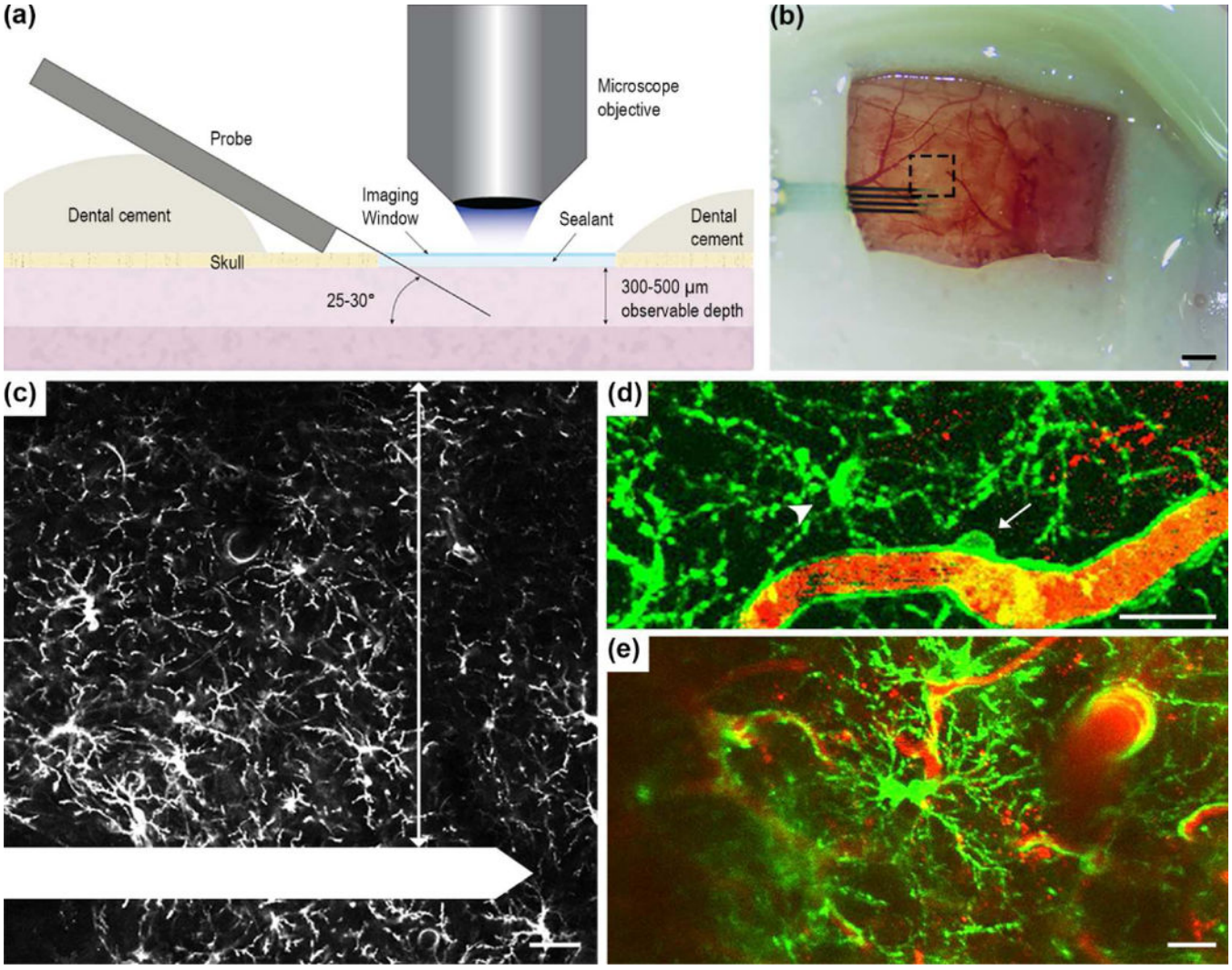

Figure 1. Experimental setup for *in vivo* tracking of NG2 glia and microglia cell dynamics

(a) Schematic of chronic imaging window preparation for two-photon microscopy. The electrode was implanted at a 25-30° angle over the mouse visual cortex, sealed with kwik-sil and a cover glass was applied over the top to preserve imaging clarity and maintain tissue health. Dental cement was used to secure the probe in place and seal the craniotomy. (b) The chronic imaging window. Black dotted box is the region of interest where z-stacks were acquired. Scale bar = 1 mm. (c) Inset of (b). NG2 glia was observed and quantified 300 µm adjacent to the electrode shank (arrow). The electrode shank is outlined in white. Scale bar = 50 µm. Both vascular bound NG2+ pericytes (d, arrow), which display distinct morphology compared to NG2 glia (d, arrowhead), and proliferating NG2 glia (e) were excluded from quantification. GFP fluorescence is labeled green and blood vessels are labeled red for (d) and (e). Scale bar = 25 µm.

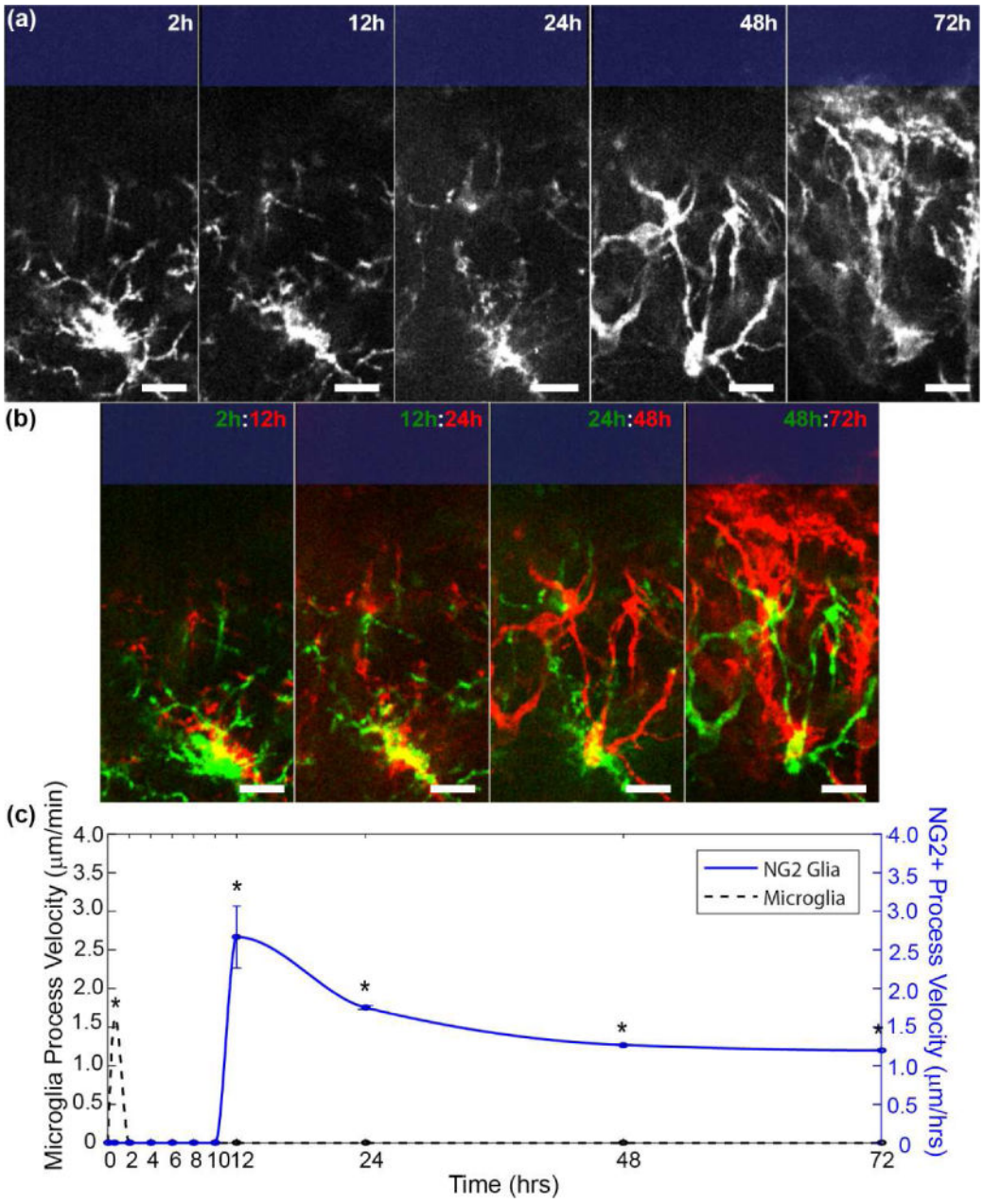

Figure 2. NG2 glia extend processes toward the probe beginning 12 hours post-insertion

(a) NG2 glia processes extend toward the probe surface (blue rectangle). Scale bar = 15 μm. (b) Merged images of NG2 glia cell. Yellow denotes where pixels before and after overlap. Red indicates extended features while green denotes retracted features. Scale bar = 15 μm. (c) NG2 glia (blue) and microglia (black dashed) process velocities were tracked over time. Velocity data for acute microglia process migration within the first hour of insertion was obtained from [34]. * indicates $p<0.05$.

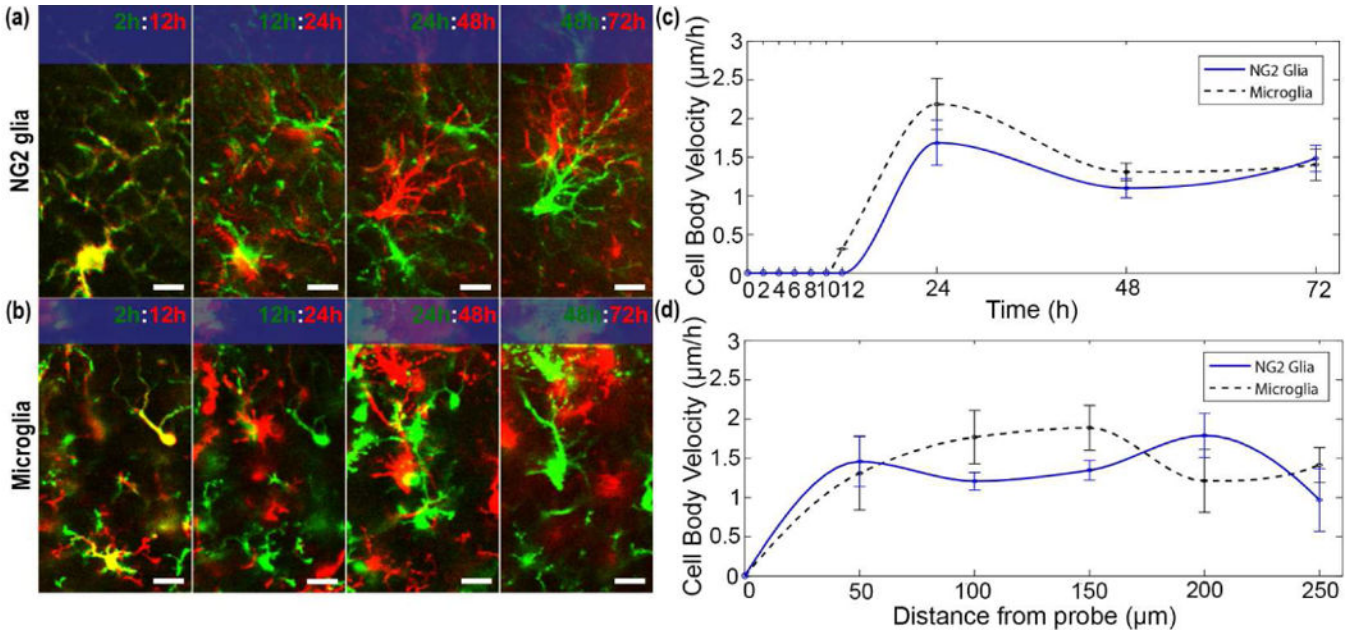

Figure 3. NG2 glia share similar kinematic patterns of cell body migration with microglia

(a) NG2 glia cells migrate toward the surface of the probe (blue rectangle) shortly after the extension of cellular processes. Green and red denotes before and after each time point, respectively. Yellow represents areas where pixels overlap, indicating no cellular movement. Scale bar = 15 μm. (b) Microglia cell body migration toward the surface of the probe (blue rectangle) over 72 hours. Scale bar = 15 μm. (c) Velocity of migrating cell bodies for NG2 glia (blue line) and microglia (black dashed) over 72 hours. (d) Cell body velocity plotted as a function of distance from the probe.

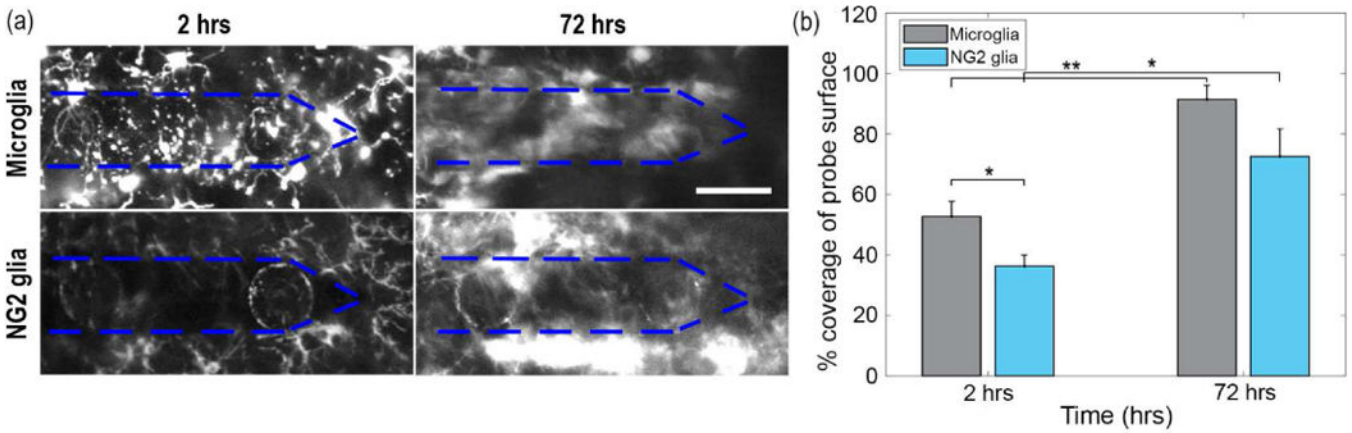

Figure 4. Coverage of cellular processes over the probe surface by NG2 glia increases following 72 hours of implantation

(a) Increases in GFP signal of NG2 glia and microglia processes over the surface of the probe from 2 hours to 72 hours post-insertion. The perimeter of the probe is outlined (blue dashed). Scale bar = 50 μm. (b) Percent of coverage over the probe surface from NG2 glia and microglia cells at 2 h and 72 h. * indicates $p < 0.05$. ** indicates $p<0.001$.

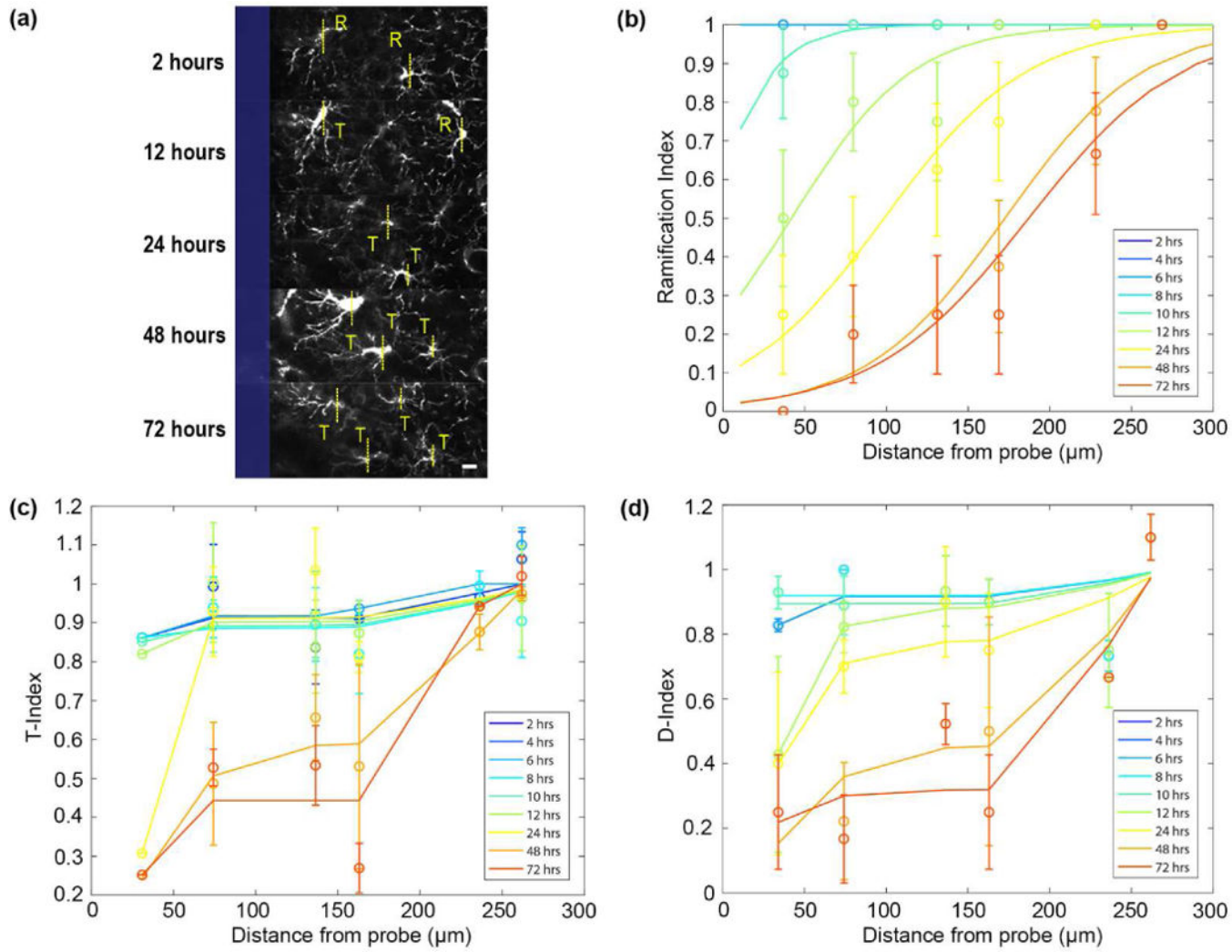

Figure 5. NG2 glia experience morphological changes 12 hours after probe insertion

(a) Classification of ramified (R) or transitional/activated (T) NG2 glia over 72 hours. The surface of the probe is outlined in blue. Scale bar = 10 μm. (b) NG2 glia ramification as a function of distance from the probe over 72 hours. NG2 glia become activated to a radius of 190.3 μm away from the surface of the probe at 72 hours. (c) Morphological index of the transitional state of NG2 glia with respect to distance from the probe (T-index). (d) Morphological index of the orientation of NG2 glia processes with respect to distance from the probe (D-index).

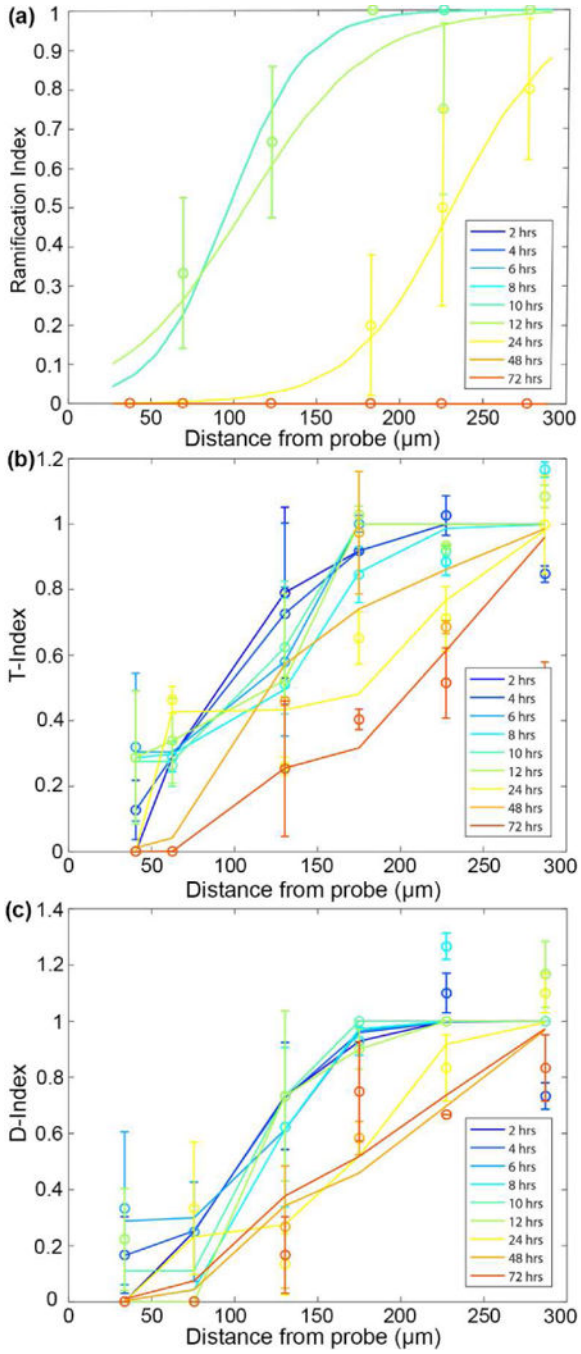

Figure 6. Distribution of microglia activation increases up to 72 hours after probe insertion

(a) Characterizing the ramification of microglia with distance from the probe surface. An index of 1 represents ramified morphology while an index of 0 represents activated, or transitional, microglia. (b) Transitional index of activated microglia where 1 represents processes extending equally in all directions and 0 represents leading processes extended toward the probe surface. (c) Directionality index of microglia where an index of 1 indicates equal number of processes extending toward and away the surface of the probe and an index of 0 indicates all processes extending toward the surface of the probe.

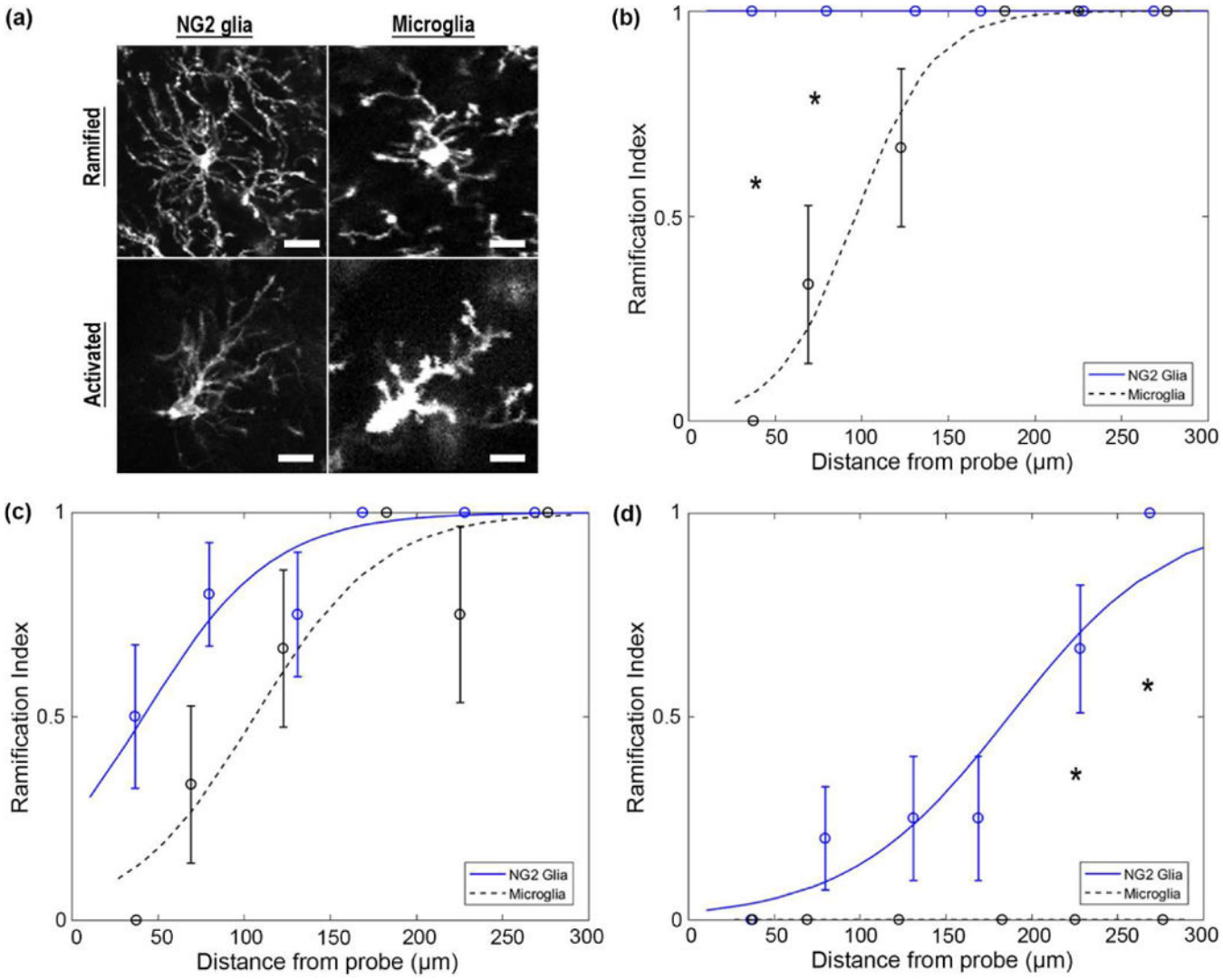

Figure 7. NG2 glia differ temporally in activation patterns compared to microglia up to 72 hours post-insertion

(a) NG2 glia express long and thin processes while microglia processes appear short and bulbous. Both cell types extend processes radially around their cell bodies when ramified and preferentially in a particular direction when activated. Scale bar = 15 μm. (b) NG2 glia and microglia have temporally different patterns of activation at 2 hours, (c) 12 hours, and (d) 72 hours post-insertion. * indicates $p<0.05$.

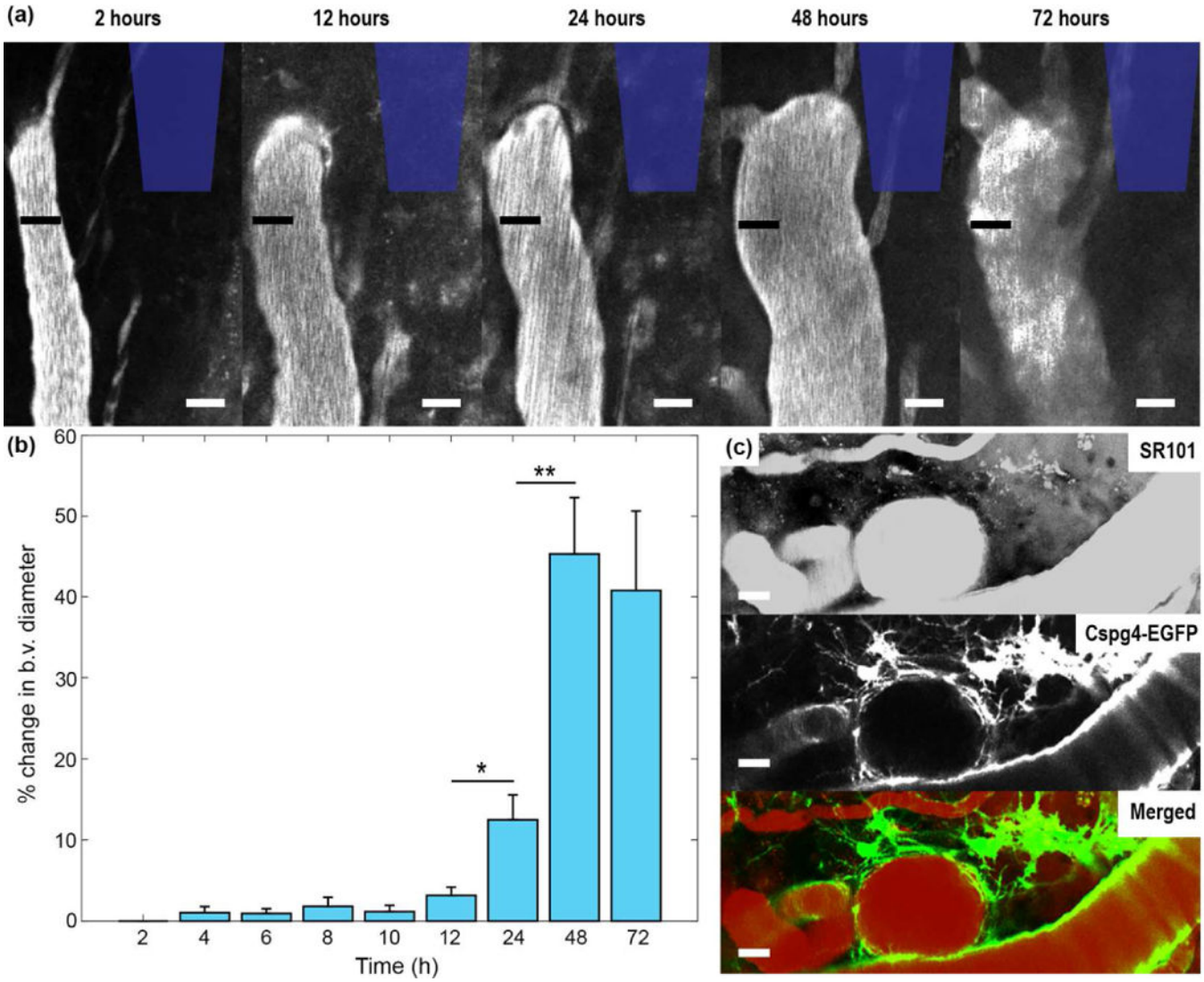

Figure 8. Vascular dynamics during inflammatory response after insertion

(a) Venuoles near the inserted probe increased in diameter over 72 hours following probe insertion. The black bar denotes the diameter of the blood vessel at 2 hours post-insertion for all time points. The position of the probe is outlined in blue. Scale bar = 25 μm. (b) Percent change in blood vessel (b.v.) diameter over time compared to original blood vessel diameter at 2 hours post-insertion. (c) NG2 glia respond to vascular events at 72 hours post-insertion. Vasculature is visualized with SR-101. Scale bar = 20 μm. * indicates $p < 0.01$. ** indicates $p<0.0001$.